The Locations of Circumpapillary Glaucomatous Defects Seen on Frequency-Domain OCT Scans

Donald C. Hood,[1,2] Diane L. Wang,[1] Ali S. Raza,[1,3] Carlos Gustavo de Moraes,[4,5] Jeffrey M. Liebmann,[4,5] and Robert Ritch[4,6]

[1]Department of Psychology, Columbia University, New York, New York
[2]Department of Ophthalmology, Columbia University, New York, New York
[3]Department of Neurobiology and Behavior, Columbia University, New York, New York
[4]Einhorn Clinical Research Center, New York Eye and Ear Infirmary, New York, New York
[5]New York University School of Medicine, New York, New York
[6]New York Medical College, Valhalla, New York

Correspondence: Donald C. Hood, Department of Psychology, 406 Schermerhorn Hall, 1190 Amsterdam Avenue, MC 5501, Columbia University, New York, NY 10027; dch3@columbia.edu

Submitted: June 26, 2013
Accepted: October 1, 2013

Citation: Hood DC, Wang DL, Raza AS, de Moraes CG, Liebmann JM, Ritch R. The locations of circumpapillary glaucomatous defects seen on frequency-domain OCT scans. *Invest Ophthalmol Vis Sci*. 2013;54:7338–7343. DOI: 10.1167/iovs.13-12680

Purpose. To examine the locations of local glaucomatous damage around the optic disc as seen in the circumpapillary retinal nerve fiber layer (RNFL) on frequency domain optical coherence tomography (fdOCT).

Methods. Optic disc fdOCT volume scans from 54 healthy control eyes and 114 patient eyes, classified as suspected or mild glaucoma, were analyzed. All patient eyes had 24-2 visual fields (VFs) with mean deviations better than −5.5 dB. By hand-correcting automated segmentation, the RNFL thickness profile was obtained for a circumpapillary circle. RNFL defects were defined as regions where the patient's RNFL thickness fell below the 99% confidence limit of control values. The location of a defect was defined as the point of greatest difference between the patient's thickness and the 99% limit. The locations of major blood vessels (BVs) were marked, and separated into superior-nasal (SN), superior-temporal (ST), inferior-temporal (IT), and inferior-nasal (IN) groups.

Results. Of the 114 patient eyes, 45 exhibited a total of 75 RNFL defects. The locations of these defects clustered around the ST, SN, and IT, but not the IN BVs.

Conclusions. The absence of defects in the IN region indicates that the locations of local defects are not simply related to either BV location or RNFL thickness. The local defects in the ST and IT regions can be related to arcuate defects seen on 24-2 and 10-2 VFs. However, the defects in the SN region suggest the presence of VF defects that may be overlooked because they fall largely outside the 24-2 test grid.

Keywords: glaucoma, optical coherence tomography, visual fields, optic disc, retinal nerve fiber layer

All regions of the optic disc are not equally sensitive to glaucomatous damage. The classic arcuate defects, seen on visual field (VF) testing, are associated with damage largely to the superior and inferior quadrants of the disc, as can be seen on fundus photographs.[1,2] Quigley et al[3] documented the relative vulnerability of the superior and inferior quadrants histologically by showing selective loss of axons in postmortem human eyes. More recently, a number of optical coherence tomography (OCT) studies demonstrated a relatively greater thinning of the retinal nerve fiber layer (RNFL) in the superior and inferior quadrants of eyes with glaucoma. [See Refs. 4 and 5 and the earlier work they reference.]

The most obvious difference among quadrants of the disc is the markedly greater thickness of the RNFL in the superior and inferior quadrants, suggesting that thicker regions may be more vulnerable to glaucomatous damage. Based on OCT optic disc volume scans of healthy individuals, we[6] recently extended a thickness hypothesis to explain the clinical observation that VF defects are relatively more severe in the upper, as compared with the lower VF,[7–10] and suggested a strong version of a thickness hypothesis. According to this hypothesis, the probability of damage at any given point of the optic disc depends on the RNFL thickness at that point or, more realistically, to some other morphological feature (e.g., pore size[11]) or biomechanical factor[12] that is correlated with RNFL thickness. To test this hypothesis, we needed to better understand how the probability or frequency of local optic disc damage varies with disc location.

Our general purpose here was to examine the locations of early glaucomatous damage in the circumpapillary RNFL as seen on OCT volume disc scans so as to better understand how the probability of local optic disc damage varies with disc location.

Methods

We analyzed 54 healthy control eyes from 54 individuals and 114 eyes from 75 patients, classified as suspected or mild glaucoma. Both groups were part of a previous study.[6] Briefly, the healthy controls had normal discs, IOPs, and VFs, and were a mean age of 53.2 ± 8.1 years, whereas the patients' mean age

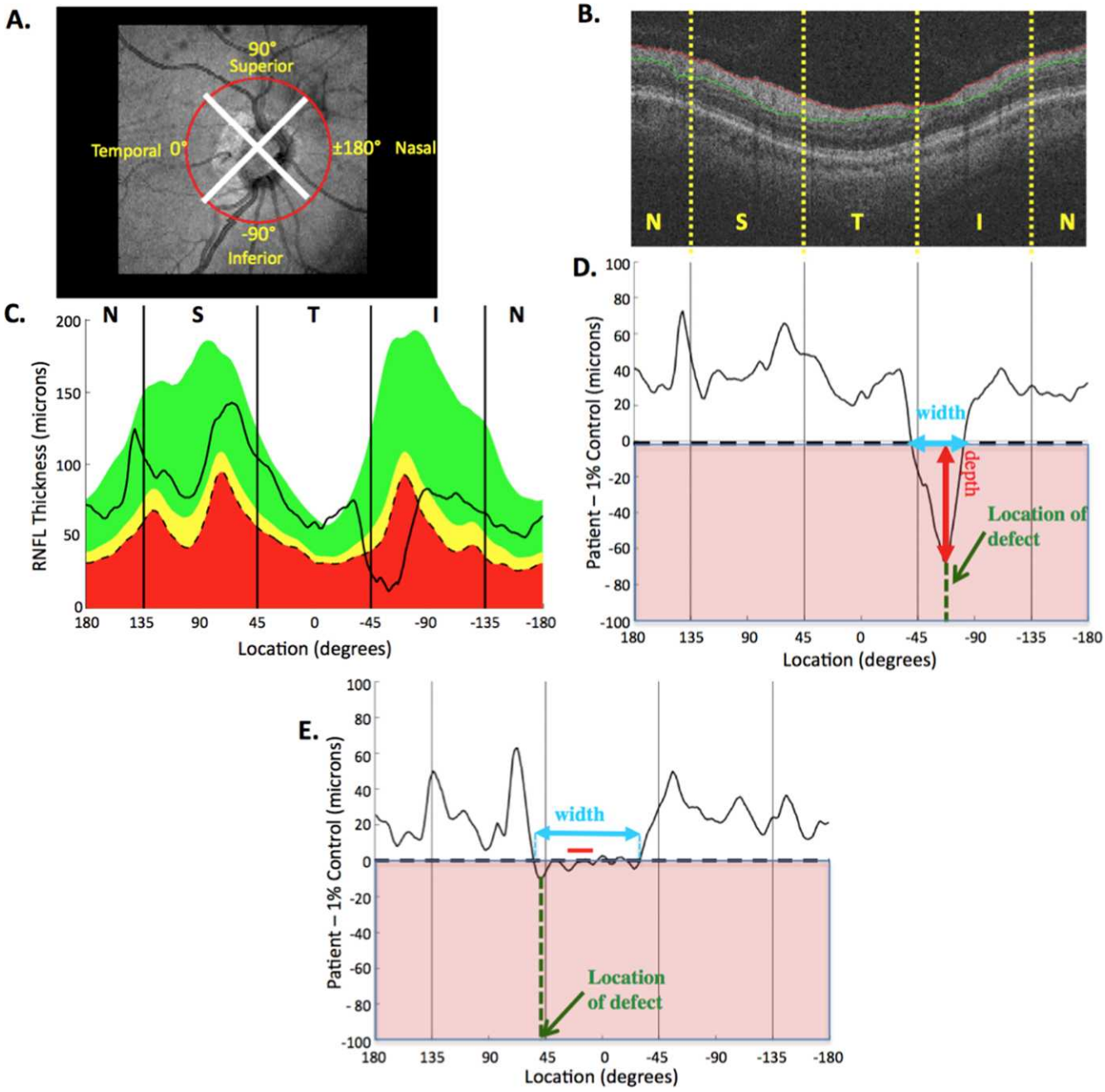

Figure 1. (**A**) Fundus view of the optic disc of a right eye showing the four quadrants and the location (*red circle*) of the OCT image in (**B**). (**B**) Circumpapillary image obtained from OCT volume scan of the disc. (**C**) The RNFL thickness (*black curve*) from the image in (**B**) shown with normal range (*green*) and 5% and 1% confidence regions, all as a function of distance around the disc. The 1% confidence limit is shown as dashed line. (**D**) The difference between RNFL thickness (*black curve* in [**C**]) and the 1% confidence limit (*dashed line* in [**C**]) is shown as a function of distance around the disc. The *pink region* corresponds to the *red region* in (**C**). (**E**) Same as in panel D for another eye. See text for details.

was 55.5 ± 12.2 years. All eyes had refractive corrections between –6.0 diopters (D) and +3.0 D. At least one eye of each patient had glaucomatous optic neuropathy (GON). GON was defined based on stereophotograph evaluation by glaucoma specialists using the following criteria: focal or diffuse neuroretinal rim thinning, focal or diffuse RNFL loss, or an intereye vertical cup-to-disc ratio asymmetry greater than 0.2 not explained by differences in disc size. All eyes had reliable 24-2 (Humphrey Visual Field Analyzer; Carl Zeiss Meditec, Inc., Dublin, CA). Because 17 of the eyes studied had superior nasal optic head defects, the stereophotographs and medical histories of these patients were scrutinized by a glaucoma expert for signs of superior segmental optic hypoplasia. In this nonprogressive congenital condition, the following signs must be present for its clinical characterization: a relative superior entrance of the central retinal artery, superior peripapillary scleral halo, pallor of the superior disc, and thinning of the superior peripapillary RNFL.[13] None of these signs were identified in these eyes.

The 114 patient eyes were selected from a larger group of 156 eyes[6] by excluding eyes with a 24-2 mean deviation (MD) that was worse than –5.5 dB ($n = 23$), eyes ($n = 2$) without OCT scans and 24-2 fields within 1 year, and an eye ($n = 1$) with a cube scan that was poorly centered. In addition, 16 eyes

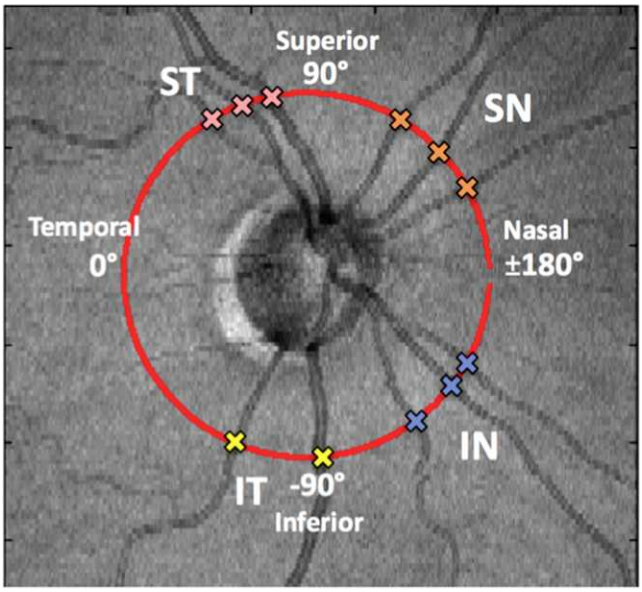

FIGURE 2. Fundus image of the optic disc of a right eye illustrating the marking of the location of the major blood vessels.

with corrections of less than –6D, were removed to match the criteria for the control group and to avoid the misidentification of a defect due to shifts in the RNFL peaks associated with the smaller axial length in myopic individuals.[14,15] Note: there was no significant difference in refractive error between the eyes with and without RNFL bundle defects.

Optic disc frequency domain OCT (fdOCT) volume scans (3D-OCT 2000; Topcon Medical Systems, Inc., Paramus, NJ) were obtained on all individuals and the image for a circumpapillary circle (Fig. 1A), 1.7 mm in radius, generated. From these circumpapillary images (Fig. 1B), RNFL thickness profiles were obtained (black curve in Fig. 1C), after segmenting the RNFL (Fig. 1B) with an automated algorithm and hand correcting as needed.[16,17]

RNFL defects were defined as circumpapillary regions where the patient's RNFL thickness fell below the 99% confidence limit of control values. To facilitate the identification and measurement of these defects, the 99% confidence limit based on all the 54 controls (black dashed curve in Fig. 1C) was subtracted from the individual patient's RNFL (black solid curve in Fig. 1C) and displayed as the black curve in Figure 1D. With this representation, the portion falling in the red region in Figure 1D (i.e., below the dashed black line) was considered abnormal. The width and depth of a defect were measured as shown in Figure 1D. The location of the defect was defined as the point with the greatest depth. Because a single defect may appear as multiple small defects (Fig. 1E), adjacent defects within 20° (red bar in Fig. 1E) were considered a single defect. To indicate the location of a defect on the circumpapillary circle (1.7-mm radius), the following convention was used in all figures, including Figure 1: 0° is the temporal most location (9 o'clock for the fundus view of the right eye); 90° the superior location (12 o'clock), –90° the inferior location (6 o'clock) and ±180° the nasal location (3 o'clock).

The locations of major blood vessels (BVs) were marked on shadowgrams as shown in Figure 2. The BVs were separated into superior-nasal (SN), superior-temporal (ST), inferior-temporal (IT), and inferior-nasal (IN) groups and their locations averaged.

RESULTS

Based on the definition above, 45 of the 114 patient eyes showed RNFL defects. These 45 eyes had a total of 75 defects with an average of 1.7 defects per eye (range 1 to 5 defects). As the blue bars in Figure 3A indicate, these 75 defects were not evenly distributed around the disc, but tended to cluster in three regions (arrows): on the border of the nasal and superior quadrants (red arrow), in the temporal portion of the superior disc (green arrow), and in the temporal portion of the inferior quadrant (blue). The vertical red lines indicate the average location of the four groups of BVs, which occurred at 132.6°, 76.2°, –75.8°, and –131.8°. Notice that the three clusters of defects roughly coincide with three of the four groups of BVs.

A similar analysis for the 54 control subjects indicated 10 RNFL "defects," presumably false positives, in 10 individuals. The 10 "defects" in the control eyes occurred in all quadrants, as indicated by the thin red bars in Figure 3A. Six of these 10 "defects" were less than 10° in width, as compared with 29% of the patients' defects. This is shown in Figure 3B, where the number of defects is plotted as a function of defect width for patients (blue) and control (red) subjects. To minimize the impact of false positives, we examined separately the defects greater than 10° in width. This left 4 defects in 54 control subjects and 56 defects for the patients.

The data for individual eyes are shown in Figure 3C, where the widths of the defects are represented as the blue horizontal lines for each of the 45 eyes (*y*-axis) with defects. The locations of the defects less than or equal to 10° and greater than 10° in width are shown as the open and filled blue circles, respectively. The locations of individual BVs are shown as the small red dots and the large open red circles show the average location of each of the four BV locations for each of the eyes. Across eyes, the BVs tended to cluster into four groups, as expected. The vertical red lines are the mean locations of these groups as in Figure 3A.

Whether one considers all 75 defects (filled and open blue circles) or only the 56 greater than 10°(filled blue circles), the conclusions are the same. First, defects occurred in all quadrants around the disc, not simply in the inferior and superior quadrants known to be at high risk. Second, the defects clustered near three of the four BV locations.

Defects also occurred in the temporal region. However, although 25 of the 56 defects greater than 10° included the temporal region, only 5 were restricted entirely to this region.

DISCUSSION

In glaucoma suspects and patients with mild VF glaucomatous defects (MD better than –5.5 dB), local defects in the circumpapillary RNFL layer were seen in all regions around the disc. However, these defects tended to cluster into three groups located close to three of the four clusters of BVs. These results raise two questions.

Why These Three Locations?

The strong version of the thickness hypothesis states that the probability of glaucomatous damage at any given point of the optic disc depends on the RNFL thickness at that point.[9] Figure 4A shows the relative circumpapillary RNFL thickness profile (black curve) for the healthy controls superimposed on the histogram (blue bars) from Figure 3A (right axis). This thickness profile was derived from the RNFL thickness map[6] in Figure 4B for the 54 healthy controls. In particular, the thickness around the black circle of 3.4 mm diameter in Figure 4B was determined and shown normalized to the peak

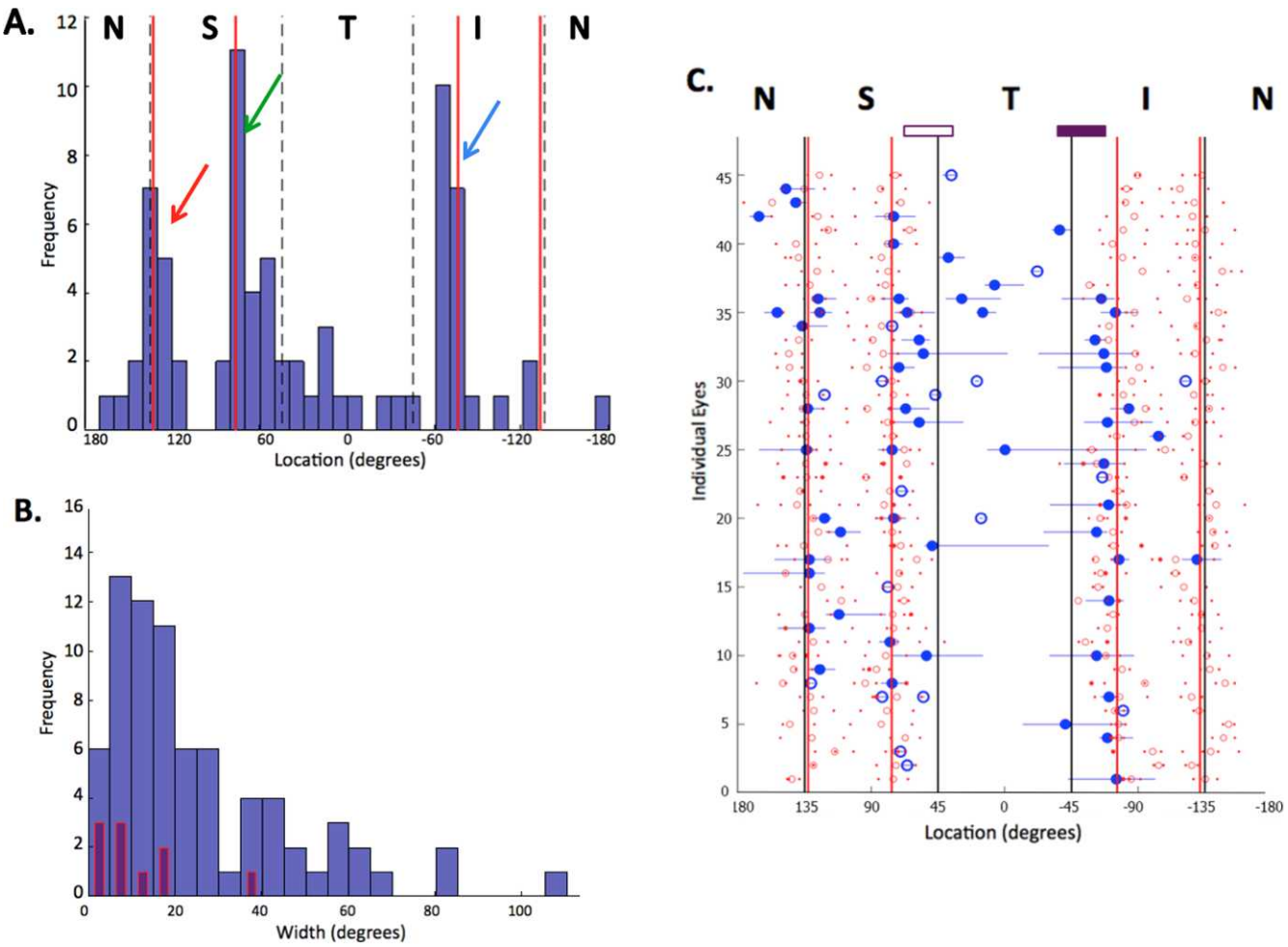

FIGURE 3. (**A**) A histogram showing the frequency of defects as a function of distance around the disc for the patients (*blue bars*) and healthy controls (*red bars*). (**B**) A histogram showing the frequency of defects of different widths for patients (*blue*) and controls (*red*). (**C**) The data for the 45 individual patient eyes with defects are arranged along the *y*-axis. The *blue circles* are the locations (see Fig. 1D) of the 75 defects with *filled* and *open* representing those greater than 10° or less than or equal to 10° in width, respectively. The *horizontal blue lines* show the extent (width) of the defect. The *small red dots* are the location of individual blood vessels and the *large open red circles* show the mean of the group of blood vessels. The *red vertical lines* are the average of the locations of the four groups of vessels. The *filled purple rectangle* shows the macular vulnerability zone[6,22] and the *open purple rectangle* the region in the superior disc at the same location. See text for details.

thickness as the solid black curve (left axis) in Figure 4A. Note that although there is a general correspondence between the frequency of defects and the RNFL thickness, this correspondence is far from perfect, especially in the regions of the IN cluster of vessels. Although the RNFL thickness in this location (black arrow) is thinner than in the other three locations showing clusters of defects, it is thicker than in many of the regions in the ST and IT areas in which many defects are located. However, one needs to be cautious in interpreting this comparison, as the peaks of the RNFL thickness profiles also include a sizable contribution from BVs.[18]

On the other hand, it appears that the scanning laser polarimetry (SLP) retardance measure of RNFL thickness has little or no contribution from BVs.[19] The dashed curve in Figure 4A shows the SLP RNFL thickness for 50 healthy controls from a previous study.[20] Although the three clusters of defects correspond to thick regions of the RNFL based on SLP, the IN (black arrow) region is also thick, but has relatively few defects. Thus, although the thickness of the RNFL may be a factor, the relationship is probably not a simple one.

There is always the possibility that this finding is artifact, due to factors not fully understood. Interestingly, Strouthidis et al.[21] found rim area loss in ocular hypertensives occurred in the IN, as well as the ST, IT, and SN regions. However, it is hard to relate their findings to ours, given that our studies differed in a number of ways, including scanning technique (Heidelberg retina tomograph versus OCT), patient population, design (progression over time versus cross-section), and measure (rim area versus RNFL thickness). In any case, there is some confirmation of our finding in a study[22] of holes (or tunnels) in the RNFL attributed to axonal drop out secondary to glaucomatous damage. These holes tended to appear in the same three regions, near the ST, SN, and IT, but not the IN BVs.

On the other hand, it is not surprising that the probability of glaucomatous damage is not dependent simply on RNFL thickness. As Burgoyne[12] recently pointed out, glaucomatous damage of retinal ganglion cell axons is likely due to a number of interacting mechanisms, including complex changes in the biomechanics of the optic disc, which may differ at different parts of the disc. Ultimately, the explanation for the pattern of

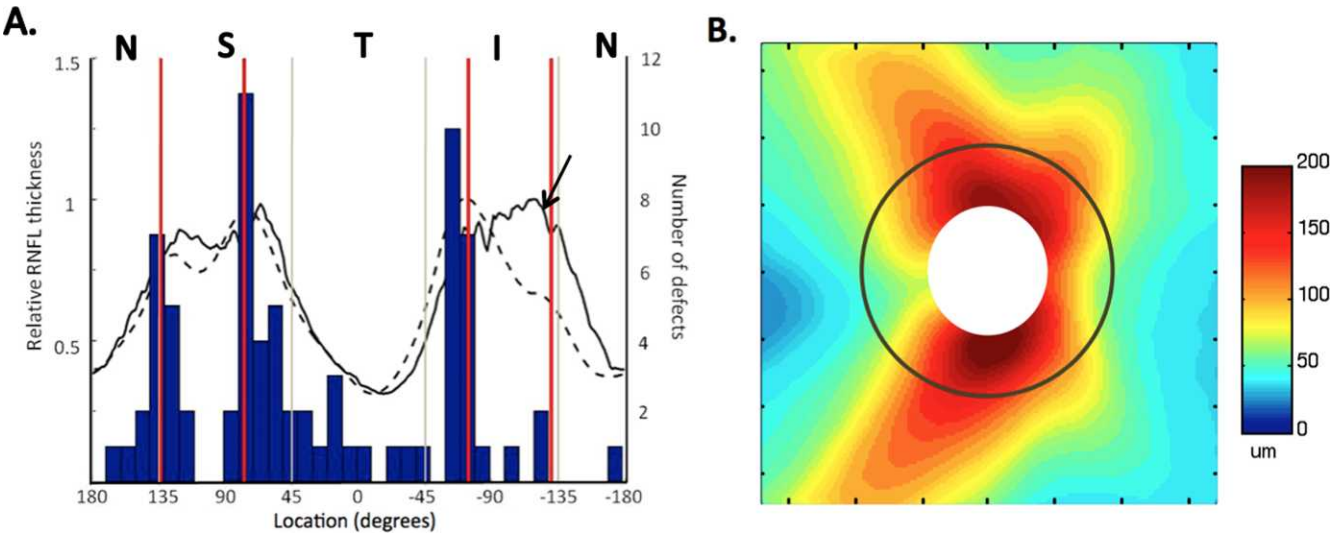

FIGURE 4. (**A**) The histogram from Figure 3A (*right axis*) is shown with the normalized average circumpapillary OCT RNFL thickness (*solid black curve*, *left axis*) for the 54 healthy control eyes and the average circumpapillary SLP RNFL thickness (*dashed black curve*, *left axis*) from 50 healthy controls reported in Reference 20. (**B**) The RNFL thickness for the optic disc cube scans from the 54 healthy controls. The *black circle* is the location of the *solid black curve* in (**A**).

defects around the disc must be sought in these mechanisms and their interactions.

Where Are the VF Defects Associated With the Three Clusters of RNFL Damage?

The cluster of defects we observe in the ST and IT regions are undoubtedly associated with the classic arcuate defects. They include the regions of the disc associated with the regions of arcuate defects seen on the 24-2 VF according to the Garway-Heath et al. map.[2,23] On 10-2 VFs, deep local arcuate defects within the central 10° are often seen in the upper VF. These defects, which can be missed on the 24-2 VF, are far less common in the lower VF. We have shown that the maximal RNFL thinning associated with these deep macular VF defects occurs in the IT regions between approximately −35° to −65° on the coordinates.[24] This region, called the macular vulnerability zone (MVZ),[6,25] is shown as the solid purple bar in Figure 3C. Note there are nearly as many defects in this region as there are in the same location of the superior disc (i.e., +35° to ±65°, open purple rectangle in Fig. 3C). However, although damage to the MVZ causes damage to the macula, damage to the ST region (open purple rectangle) falls outside the macula due to the asymmetric nature of the macula to disc connections.[24,25]

On the other hand, the defects associated with the thinning in the SN region ought to fall largely outside even the 24-2 VF.[2,26] It is well known that defects can fall outside the center 24° of the visual field, as seen, for example, on kinetic perimetry.[27,28] Further, peripheral defects have been reported in patients whose central VFs were categorized as normal on standard static perimetry.[29–32] However, the relationship between these peripheral defects and the local defects we see at the SN disc requires further study.

Limitations

By design, this study focused on clear local thinning of the RNFL. Consequently, shallow damage might be missed by our procedures. Or, put a different way, we do not know the false-negative (miss) rate of our technique when it comes to detecting glaucoma, although determining sensitivity, or specificity, was not the purpose here. In other words, there are probably eyes in this study with glaucomatous damage that are not included in the 55 eyes with local defects. However, this limitation has minimal impact on our two main conclusions. First, it does not affect our conclusion that there are defects in the SN portion of the disc. Second, even in the unlikely event that these shallow defects showed a better correspondence with RNFL thickness or BV locations, one would have to assume that these factors predict the frequency of occurrence, but not the depth, of damage in order to rescue the thickness or BV hypotheses.

A second limitation concerns the definition of a local defect. The variability in RNFL thickness among healthy individuals is not constant around the disc. Therefore, a fixed amount of thinning will not be equally detectable at all disc locations. For this reason, we defined abnormal RNFL thinning based on the 99% confidence limit of healthy controls. However, there is no "right" way to take variability into consideration and we cannot rule out the possibility that a different method of controlling for normal variability would produce a different result.

A related problem concerns the relation of the depth of a local RNFL defect and the loss of associated retinal ganglion cell (RGC) axons. Whether depth is taken as the difference from the mean of controls or the difference below the 99% confidence limit, we cannot assume that a constant loss in RNFL thickness equals a constant loss in number of RGC axons. In fact, given that the width of the RGC axon is smaller in the macula than the more peripheral regions of the retina, OCT RNFL measures may underestimate the number of axons damaged in the portion of the disc associated with the macula (i.e., the temporal quadrant and temporal portion of the inferior quadrant).

Summary

Local glaucomatous damage is not equally distributed around the optic disc, nor is this damage simply related to either BV location or RNFL thickness. Further, the damage identified in the SN portion of the disc may fall outside the region covered by the 24-2 VF. Eyes with RNFL defects seen at this location

may require broader field perimetry if one aims to document functional damage.

Acknowledgments

Supported by National Institutes of Health Grant R01-EY-02115 (DCH) and a grant of equipment from Topcon, Inc.

Disclosure: **D.C. Hood**, Topcon, Inc. (F, C); **D.L. Wang**, None; **A.S. Raza**, None; **C.G. de Moraes**, None; **J.M. Liebmann**, None; Topcon, Inc. (F, C); **R. Ritch**, None

References

1. Hoyt WF, Frissen L, Newman NM. Fundoscopy of nerve fiber layer defects in glaucoma. *Invest Ophthalmol Vis Sci*. 1973;12:814–829.
2. Garway-Heath DF, Poinoosawmy D, Fitzke FW, Hitchings RA. Mapping the visual field to the optic disc in normal tension glaucoma eyes. *Ophthalmology*. 2000;107:1809–1815.
3. Quigley HA, Addicks EM, Green WR. Optic nerve damage in human glaucoma. III. Quantitative correlations of nerve fiber loss and visual field defect in glaucoma, ischemic neuropathy, papilledemia, and toxic neuropathy. *Arch Ophthalmol*. 1988;100:135–146.
4. Leite MT, Zangwill LM, Weinreb RN, et al. Structure-function relationships using the Cirrus spectral domain optical coherence tomograph and standard automated perimetry. *J Glaucoma*. 2012;21:49–54.
5. Rao HL, Babu JG, Addepalli UK, Senthil S, Garudadri CS. Retinal nerve fiber layer and macular inner retina measurements by spectral domain optical coherence tomograph in Indian eyes with early glaucoma. *Eye*. 2012;26:133–139.
6. Hood DC, Raza AS, de Moraes CGV, et al. The nature of macular damage in glaucoma as revealed by averaging optical coherence tomography data. *Trans Vis Sci Technol*. 2012;1:1–15.
7. Nicholas SP, Werner EB. Location of early glaucomatous visual field defects. *Can J Ophthalmol*. 1980;15:131–133.
8. Drance SM. The visual field of low tension glaucoma and shock induced optic neuropathy. *Arch Ophthalmol*. 1977;95:1359–1361.
9. Heijl A, Lundqvist L. The frequency distribution of earliest glaucomatous visual field defects documented by automatic perimetry. *Acta Ophthalmol*. 1984;62:658–664.
10. Lewis RA, Phelps CD. A comparison of visual field loss in primary open angle glaucoma and the secondary glaucomas. *Ophthalmologica*. 1984;189:41–48.
11. Quigley HA, Addicks EM. Regional differences in the structure of the lamina cribrosa and their relation to glaucomatous optic nerve damage. *Arch Ophthalmol*. 1981;99:137–143.
12. Burgoyne CF. A biomechanical paradigm for axonal insult within the optic nerve head in aging and glaucoma. *Exp Eye Res*. 2011;93:120–132.
13. Kim RY, Hoyt WF, Lessell S, Narahara MH. Superior segmental optic hypoplasia. A sign of maternal diabetes. *Arch Ophthalmol*. 1989;107:1312–1315.
14. Yoo YC, Lee CM, Park JH. Changes in peripapillary retinal nerve fiber layer distribution by axial length. *Optom Vis Sci*. 2012;89:4–11.
15. Yamashita T, Asaoka R, Tanaka M, et al. Relationship between position of peak retinal nerve fiber layer thickness and retinal arteries on sectoral retinal nerve fiber layer thickness. *Invest Ophthalmol Vis Sci*. 2013;54:5481–5488.
16. Yang Q, Reisman CA, Wang Z, et al. Automated layer segmentation of macular OCT images using dual-scale gradient information. *Optics Express*. 2010;18:21293–21307.
17. Raza AS, Cho J, De Moraes CG, et al. Retinal ganglion cell layer thickness and local visual field sensitivity in glaucoma. *Arch Ophthal*. 2011;129:1529–1536.
18. Hood DC, Fortune B, Arthur SN, et al. Blood vessel contributions to retinal nerve fiber layer thickness profiles measured with optical coherence tomography. *J Glaucoma*. 2008;17:519–528.
19. Huang XR, Bagga H, Greenfield DS, Knighton RW. Variation of the peripapillary retinal nerve fiber layer birefringence in normal human subjects. *Invest Ophthalmol Vis Sci*. 2004;45:3073–3080.
20. Hood DC, Salant JA, Arthur SN, et al. The location of the inferior and superior temporal blood vessels and interindividual variability of the retinal nerve fiber layer thickness. *J Glaucoma*. 2009;19:158–166.
21. Strouthidis NG, Gardiner SK, Sinapis C, et al. The spatial pattern of neuroretinal rim loss in ocular hypertension. *Invest Ophthalmol Vis Sci*. 2009;50:3737–3742.
22. Xin D, Talamini CL, Raza AS, et al. Hypodense regions ("holes") in the retinal nerve fiber layer in frequency-domain OCT scans of glaucoma patients and suspects. *Invest Ophthalmol Vis Sci*. 2011;52:7180–7186.
23. Hood DC, Kardon RH. A framework for comparing structural and functional measures of glaucomatous damage. *Prog Retin Eye Res*. 2007;26:688–710.
24. Hood DC, Raza AS, de Moraes CG, et al. Initial arcuate defects within the central 10 degrees in glaucoma. *Invest Ophthalmol Vis Sci*. 2011;52:940–946.
25. Hood DC, Raza AS, de Moraes CG, Liebmann JM, Ritch R. Glaucomatous damage of the macula. *Prog Retin Eye Res*. 2013;32:1–21.
26. Jansonius NM, Nevalainen J, Selig B, et al. A mathematical description of nerve fiber bundle trajectories and their variability in the human retina. *Vis Res*. 2009;49:2157–2163.
27. Aulhorn E, Harms M. Early visual field defects in glaucoma. In: Leydhecker W, ed. *Glaucoma: Tutzing Symposium*. Basel: Karger; 1967:151–186.
28. Drance SM. Some studies of the relationships of hemodynamics and ocular pressure in open-angle glaucoma. *Trans Ophthalmol Soc U K*. 1969;88:633–640.
29. LaBlanc RP. Peripheral nasal field defects. *Doc Ophthalmol*. 1976;14:131–133.
30. Stewart WC, Shields MB. The peripheral visual field in glaucoma: reevaluation in the age of automated perimetry. *Surv Ophthalmol*. 1991;36:59–69.
31. Ballon BJ, Echelman DA, Shields MB, Ollie AR. Peripheral visual field testing in glaucoma by automated kinetic perimetry with the Humphrey Field Analyzer. *Arch Ophthalmol*. 1992;110:1730–1732.
32. Bellios N, Horn FK, Lammer R, et al. Uberschwellige periphere Stimulation bei praperimetrischen Glaukomen. *Ophthalmologe*. 2008;105:656–660.

Investigative Ophthalmology & Visual Science